Characterization of bulk and surface currents in strain-balanced InGaAs quantum-well mesa diodes

C. Kelleher, R. Ginige, and B. CorbettG. Clarke

Citation: Appl. Phys. Lett. **85**, 6033 (2004); doi: 10.1063/1.1835537
View online: http://dx.doi.org/10.1063/1.1835537
View Table of Contents: http://aip.scitation.org/toc/apl/85/24
Published by the American Institute of Physics

Characterization of bulk and surface currents in strain-balanced InGaAs quantum-well mesa diodes

C. Kelleher,[a] R. Ginige, and B. Corbett
NMRC, Prospect Row, Cork, Ireland

G. Clarke
IQE, Cypress Drive, St.Mellons,Cardiff, Wales, United Kingdom CF3 OEG

(Received 12 April 2004; accepted 29 October 2004)

We compare the electrical and optical characteristics of mesa diodes based on $In_{0.62}Ga_{0.38}As/In_{0.45}Ga_{0.55}As$ strain-balanced multiple-quantum wells (SB-MQW) with lattice-matched (LM) $In_{0.53}Ga_{0.47}As$ diodes. The dark current density of the SB-MQW devices is at least an order of magnitude lower than the LM devices for voltages >0.4 V. Sidewall recombination current is only measured on SB-MQW diodes when exposed to a damaging plasma. While radiative recombination current dominates in the SB-MQW diodes, it is less than the diffusive current in the LM diodes for the same applied voltage. © *2004 American Institute of Physics*. [DOI: 10.1063/1.1835537]

Thermo-photovoltaic (TPV) conversion[1] is an emerging technology that enables electrical power to be generated from a combustion process. Light emitted from a heat source in the temperature range 1500–1800 K requires absorbers with band gap energies <1 eV to generate power. These heat sources can be used to thermally excite emitters based on erbium and holmium which selectively emit light around 1.5 and 1.9 μm, respectively.[2] In order to achieve efficient absorption and conversion at the longer wavelength we have developed strain-balanced *p-i-n* InGaAs multiple-quantum wells (SB-MQWs)[3–5] with an absorption edge of 1.76 μm (0.705 eV) compared with 1.65 μm (0.75 eV) for lattice-matched (LM) abrupt *p-n* junction structures.[6] Under forward bias the emission is peaked at the band edge.

In this letter we compare the electrical and optical characteristics of mesa-isolated devices based on SB and LM structures as shown in Fig. 1. We used selective wet etching to fabricate mesa-isolated diodes ranging in radius from 68 to 750 μm. We measured the forward dark current–voltage ($I-V$) characteristics of the diodes as a function of the mesa diameter and extracted the ideality factor, n, as a function of voltage using the standard diode equation

$$I = I_0\left[\exp\left(\frac{qV}{nkT}\right) - 1\right], \tag{1}$$

where I_0 is the reverse saturation current, q the elementary charge, k is the Boltzmann constant, and T the absolute temperature.

As in all photovoltaic cells the dark current acts against the photogenerated current and should be reduced. In Figs. 2(a) and 2(b) we compare the dark current density, $J-V$ and $n-V$ of the SB-MQW with the LM diodes. The ideality for the LM diode is seen to be near "ideal," i.e., $n=1$, for voltages between 0.25 and 0.5 V. The increase in n, observed at the higher voltages, is due to carrier "pileup"[7] giving rise to a pseudo $n=2$ regime. For the SB-MQW different recombination mechanisms dominate at different voltages as the carrier density increases which in turn alters the extracted ideality factor. At low bias ($V<0.3$ V) the ideality factor is characteristic of a combination of radiative and nonradiative behavior due to defect-mediated recombination or an imbalance between electron and hole densities. As the bias increases, n approaches 1 indicative of radiatively dominated recombination. We note that the current density of the SB-MQW mesa diode is lower than the LM mesa diode. For example, at 0.4 V, where an ideality of 1 is dominant, $J_{(LM)}=0.17$ A/cm^2 and $J_{(MQW)}=0.01$ A/cm^2 for the LM and SB-MQW devices, respectively. The extracted reverse saturation current density (J_0) for the LM structure is 8×10^{-8} A/cm^2 which is in reasonable agreement with the theoretical value of 4×10^{-8} A/cm^2 derived using the equation

$$J_0 = n_i^2 q\left(\frac{D_n}{N_A L_n} + \frac{D_p}{N_D L_p}\right), \tag{2}$$

where n_i is the intrinsic carrier concentration and D_n, L_n and D_p, L_p are the diffusion constants and diffusion lengths for electrons and holes, respectively. For $In_{0.53}Ga_{0.47}As$, $n_i=8.3$

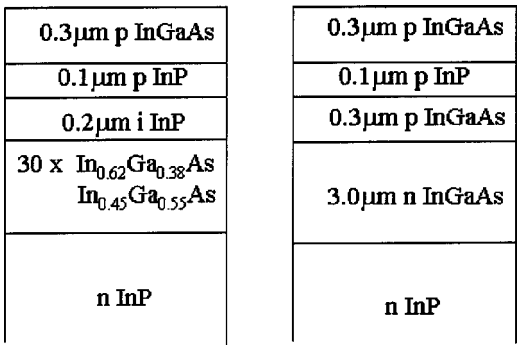

FIG. 1. Schematic layer composition and thicknesses of (a) SB-MQW and (b) LM structures. The MQW absorbing region consists of 30 repeats of 12-nm-thick $In_{0.62}Ga_{0.38}As$ compressively strained wells balanced by 12-nm-thick $In_{0.45}Ga_{0.55}As$ tensile barrier layers. X-ray diffraction measurements showed a superlattice period of 21 nm rather than the nominal 24 nm. The doping levels in the LM for p- and n-type InGaAs are 8×10^{18} and 4×10^{17} cm^{-3}, respectively.

[a]Author to whom correspondence should be addressed; electronic mail: carmel.kelleher@nmrc.ucc.ie

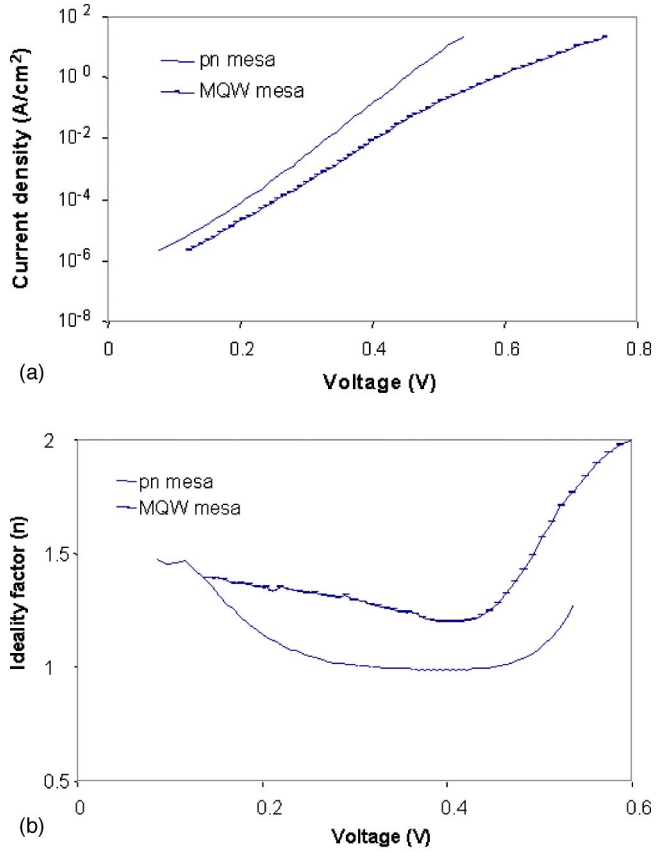

FIG. 2. (a) Forward dark current density-voltage characteristic for a LM and SB-MQW pin mesa diodes each with a radius of 380 μm. (b) Extracted electrical ideality vs voltage for a LM and a SB-MQW mesa diode each of radius 380 μm.

$\times 10^{11}$ cm^{-3},[8] $D_n = 181$ cm^2 s^{-1}, $D_p = 6.2$ cm^2 s^{-1}, $L_n = 1.1$ μm and $L_p = 3.8$ μm. L_n is limited in this case to 0.7 μm by the thin cap layers.

For the SB-MQW diode there are contributions to the dark current due to carrier diffusion from the InP cladding layers and to generation-recombination currents in the MQW region.[9] In our case the dark current is dominated by radiative recombination (see below) with $J_{0(\mathrm{MQW})} = qBdn^2_{i(\mathrm{MQW})}$ where $n_{i(\mathrm{MQW})}$ is the intrinsic carrier density in the MQW region, B is the radiative recombination coefficient (10^{-10} cm^3/s) and d is the thickness of the quantum well region. Ascribing all the current to radiative recombination implies $n_{i(\mathrm{MQW})}$ is 2×10^{12} cm^{-3}. However, this is an overestimate, as interfacial recombination will also contribute. This expression assumes equal electron and holes in all wells which is expected to improve as the carrier density increases.

To determine the effect of perimeter recombination resulting from device processing, we studied the I–V characteristics of the mesa diodes before and after exposing the unpassivated mesa sidewalls to an oxygen plasma (10 min at 80 W), a typical process encountered during device processing. After exposure to the plasma, an increase in the dark current at voltages below 0.5 V was measured in the SB-MQW devices. No change was measured for higher voltages or for the *p-n* devices though sidewall leakage could be masked by the higher dark current in that case.

Figure 3 shows the current density at 0.4 V versus the inverse of the radius of the SB-MQW devices before and after the oxygen plasma treatment. The surface recombination velocity, S, can be extracted[10] from this data. If the bulk nonradiative recombination can be neglected, as is the case at $V = 0.4$ V, the surface recombination current density, J_{rec}, can be expressed as

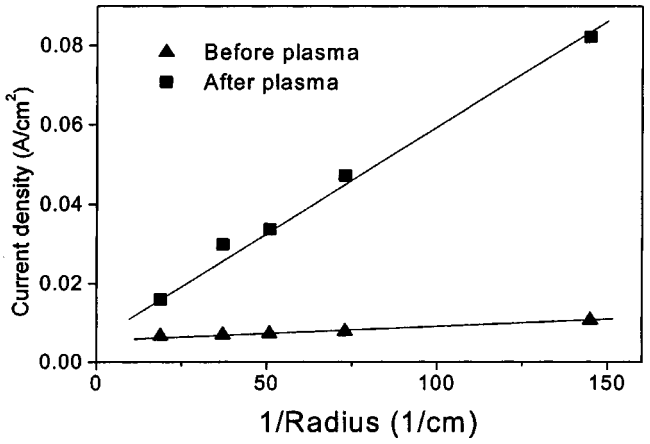

FIG. 3. Current density at a voltage of 0.4 V vs inverse radius before and after oxygen plasma treated at 80 W for 10 min for SB-MQW mesa diodes. It is seen that after plasma damage the surface recombination is significant at $V = 0.4$ V for devices of radius less than 500 μm.

$$J_{\mathrm{rec}} = \frac{2qn_i dS}{R} \exp\left(\frac{qV}{2kT}\right), \tag{3}$$

where R is the radius of the diode. Using the above expressions with the estimated effective $n_{i(\mathrm{MQW})}$, S is estimated to be 5×10^3 cm/s after the plasma treatment. Prior to the plasma damage this implies S is $\sim 3 \times 10^2$ cm/s. As this value is lower than values found by other methods[11] it suggests that the effective $n_{i(\mathrm{MQW})}$ is lower or that the thickness (d) that contributes to the recombination is less than the full thickness of the intrinsic region. To further verify the cause of the increased current the SB-MQW mesa sidewalls were etched in a mixture of H_2O_2:H_3PO_4:H_2O in the ratio of 1:1:8 for 30 s. On remeasuring, the current returned to its original value.

Figure 4 is a plot of the measured light–current (L–I) characteristics from our devices and shows that radiative recombination dominates in the SB-MQW device. The L–I is linear for both structures up to 50 mA or 3 A/cm^2. This

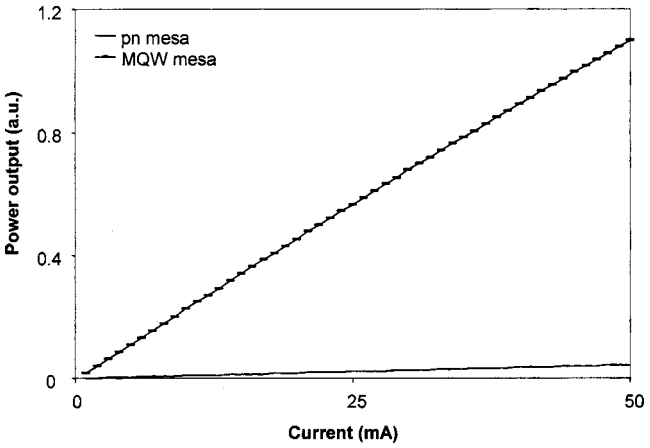

FIG. 4. Light current characteristic for LM and SB-MQW pin mesa diodes of radius 750 μm. The light is measured through the transparent InP substrate.

measurement demonstrates that the higher n value extracted for the SB-MQW from the $I-V$ characteristics does not preclude radiative recombination ($n=1$) from being the dominant mechanism in the voltage range of interest. The higher light output in the SB-MQW can be explained by a combination of a larger intrinsic region and a higher carrier density at a given current. It is also clear that the current in the case of the LM abrupt junction structure, which has an electrical ideality of 1, is dominated by the diffusion of carriers and their collection across the junction.

In conclusion, we have shown that our SB-MQW based structures with an extended absorption range have a reduced dark current for a given voltage in comparison with LM structures. As this dark current is proportional to the thickness of the quantum well region it suggests that minimizing the well and barrier thickness is desired in making SB-MQW devices superior in TPV applications. An electrical ideality factor of 1 is associated with a diffusive current for the LM structure and by radiative recombination in the case of the SB-MQW structure. We have shown that care needs to be taken in device processing, particularly with SB-MQW devices where a surface recombination current can be introduced by plasma damage. Optimization of device performance can benefit from the introduction of a plasma damage removal step.

This work was funded in part by the European Union (Project No. NNE5-1999-00573) and the Irish HEA through the PRTLI fund.

[1]T. J. Coutts and M. C. Fitzgerald, Sci. Am. **79**, 90 (1998).
[2]A. Licciulli, D. Diso, G. Torsello, S. Tundo, A. Maffezzoli, M. Lomascolo, and M. Mazzer, Semicond. Sci. Technol. **18**, S174 (2003).
[3]N. J. Ekins-Daukes, K. W. J. Barnham, J. P. Connolly, J. S. Roberts, J. C. Clark, G. Hill, and M. Mazzer, Appl. Phys. Lett. **75**, 4195 (1999).
[4]C. Rohr, J. P. Connolly, N. Ekins-Daukes, P. Abbott, I. Ballard, K. Barnham, M. Mazzer, and C. Button, Physica E (Amsterdam) **14**, 158, (2002).
[5]J. C. Dries, M. R. Gokhale, K. J. Thomson, S. R. Forrest, and R. Hull, Appl. Phys. Lett. **73**, 2263 (1998).
[6]D. M. Wilt, N. S. Fatemi, P. P. Jenkins, V. G. Weizer, R. W. Hoffman, Jr., R. K. Jain, C. S. Murray, and D. R. Riley, Thermophotovoltaic Generation of Electricity, Third NREL Conference, AIP Conf. Proc. **401**, 237 (1997).
[7]R. Ginige, K. Cherkaoui, V. Wong Kwan, C. Kelleher, and B. Corbett, J. Appl. Phys. **95**, 2809 (2004).
[8]M. Illegens, *Properties of Lattice Matched and Strain Balanced InGaAs* (Inspec, IEEE, London. 1993), p. 23.
[9]B. Corbett and W. M. Kelly, Appl. Phys. Lett. **62**, 87 (1993).
[10]N. G. Anderson, J. Appl. Phys. **78**, 1850 (1995).
[11]H. Ichikawa, K. Inoshita, and T. Baba, Appl. Phys. Lett. **78**, 2119 (2001).